Mon. Not. R. Astron. Soc. **000**, 1–14 (2008) Printed 4 July 2008 (MN LATEX style file v2.2)

arXiv:0807.0758v1 [astro-ph] 4 Jul 2008

The non-dipolar magnetic fields of accreting T Tauri stars

S. G. Gregory[1]⋆, S. P. Matt[2], J.-F. Donati[3] and M. Jardine[1]
[1] *SUPA, School of Physics and Astronomy, University of St Andrews, North Haugh, St Andrews, Fife, KY16 9SS*
[2] *Department of Astronomy, University of Virginia, P.O. Box 400325, Charlottesville, VA 22904-4325, USA*
[3] *Laboratoire d'Astrophysique, Observatoire Midi-Pyrénées, 14 Av. E. Belin, F-31400 Toulouse, France*

ABSTRACT

Models of magnetospheric accretion on to classical T Tauri stars often assume that stellar magnetic fields are simple dipoles. Recently published surface magnetograms of BP Tau and V2129 Oph have shown, however, that their fields are more complex. The magnetic field of V2129 Oph was found to be predominantly octupolar. For BP Tau the magnetic energy was shared mainly between the dipole and octupole field components, with the dipole component being almost four times as strong as that of V2129 Oph. From the published surface maps of the photospheric magnetic fields we extrapolate the coronal fields of both stars, and compare the resulting field structures with that of a dipole. We consider different models where the disc is truncated at, or well-within, the Keplerian corotation radius. We find that although the structure of the surface magnetic field is particularly complex for both stars, the geometry of the larger scale field, along which accretion is occurring, is somewhat simpler. However, the larger scale field is distorted close to the star by the stronger field regions, with the net effect being that the fractional open flux through the stellar surface is less than would be expected with a dipole magnetic field model. Finally, we estimate the disc truncation radius, assuming that this occurs where the magnetic torque from the stellar magnetosphere is comparable to the viscous torque in the disc.

Key words: Stars: pre-main sequence – Stars: magnetic fields – Stars: coronae – Stars: activity – Xrays: stars – Stars: individual: BP Tau, V2129 Oph

1 INTRODUCTION

Classical T Tauri stars (cTTSs) are young solar analogs which are accreting material from circumstellar discs. Many observations are consistent with the scenario of the stellar field truncating the inner disc and channelling gas onto discrete regions of the stellar surface. The shapes of near-IR spectral energy distributions (e.g. Robitaille et al. 2007), and the kinematics of CO lines formed in the disc (Najita, Carr & Mathieu 2003), are consistent with the disc having been truncated at a distance of a few stellar radii. Average surface fields of order a kG have been detected on a number of cTTSs (Johns-Krull 2007), which models suggest will be strong enough to disrupt the inner disc (Königl 1991). The detection of inverse P-Cygni profiles, with widths of several hundred kms^{-1}, can also be explained by material essentially free-falling along the field lines of the stellar magnetosphere from the location of the inner disc (Edwards et al. 1994). Furthermore, the excess continuum emission (veiling) in the optical and UV is likely to arise from shocks at the base of accretion funnels, with emission lines with high excitation potentials, e.g. HeI 5876Å, forming mainly in such regions (Beristain et al. 2001).

The magnetic interaction between the stellar field and the disc may also have important consequences for the formation of planets. Simulations by Romanova & Lovelace (2006), and analytic work by Lin, Bodenheimer & Richardson (1996) and Fleck (2008), suggest that the inner disc hole, cleared by the star-disc interaction, may provide a natural barrier that decreases the rate of inward migration of forming planets. There is also evidence that the large scale magnetosphere may directly disrupt the inner disc, producing warps which in some systems cross the observer's line-of-sight to the star (e.g. AA Tau, Bouvier et al. 2007). Indeed 3D MHD simulations have demonstrated that complicated warping effects in the disc truncation region may be common for T Tauri stars (Romanova et al. 2003, 2004).

The star-disc interaction may also explain the slower rotation of cTTSs compared to the typically older weak-line T Tauri stars, whose discs have largely dispersed (see e.g. the review by Bouvier 2007). Accretion of material from the inner disc would act to spin-up the central star in the absence of some physical mechanism to remove angular momentum from the system. Various magnetospheric accretion

---

⋆ E-mail: sg64@st-andrews.ac.uk

models have been developed to explain this mechanism, which differ in their assumed location of the inner disc, the details of how angular momentum is removed, and how the magnetic field topology controls both accretion and outflows (Königl 1991; Collier Cameron & Campbell 1993; Shu et al. 1994; Ferreira, Pelletier & Appl 2000; Ferreira, Dougados & Cabrit 2006; Küker, Henning & Rüdiger 2003; Matt & Pudritz 2005a,b, 2008a,b; Long, Romanova & Lovelace 2005; Bessolaz et al. 2008). Although observations indicate that the magnetic field topologies of cTTSs are complex (e.g. see the discussion in Gregory et al. 2006a), the majority of accretion models simply assume that the star has a strong dipolar magnetic field. Recently however a few studies have dropped this assumption, with Gregory et al. (2005, 2006a) and Jardine et al. (2006) being the first to consider how magnetic fields with a realistic degree of complexity would affect the accretion process. Other field geometries have since been considered by Long, Romanova & Lovelace (2007, 2008) who present the results of a 3D MHD simulation of accretion to stars with composite fields that consist of dipole and quadrupole components tilted at various angles relative to the stellar rotation axis.

It is only recently, however, that instrumentation has advanced to the stage where it is possible to map the magnetic topologies of classical T Tauri stars. Donati et al. (2007, 2008a) have recently published magnetic surface maps derived from Zeeman-Doppler imaging of the young solar-analogs V2129 Oph and BP Tau, using data from the ESPaDOnS and NARVAL spectropolarimeters at the Canada-France-Hawai'i Telescope and Télescope Bernard Lyot respectively. Using the pre-main sequence evolutionary model of Siess, Dufour & Forestini (2000), Donati et al. (2007) determined that V2129 Oph, a high-mass T Tauri star of $1.35\,\mathrm{M}_\odot$, had developed a radiative core. In contrast, BP Tau, at $0.7\,\mathrm{M}_\odot$, should be completely convective (Donati et al. 2008a). As the internal structure, and therefore the magnetic field generation process, is different in both V2129 Oph and BP Tau, it is of particular interest to compare the structure and properties of their magnetic fields, as well as comparing both to a dipole.

In §2 we summarise the stellar parameters and magnetic field measurements of BP Tau and V2129 Oph. In §3 we describe how three-dimensional coronal fields can be extrapolated from Zeeman-Doppler maps of photospheric magnetic fields, and compare the resulting field topologies with a large scale dipole. In §4 and §5 we discuss the structure of the open stellar, and accreting, field, while §6 contains our conclusions.

2 THE STARS BP TAU AND V2129 OPH

BP Tau is one of the best studied classical T Tauri stars, with an abundance of observational data across most wavebands. In contrast to this, V2129 Oph is less well studied, despite being the brightest T Tauri star in the ρ-Oph star forming cloud.

2.1 Stellar parameters

For BP Tau we adopt the same stellar parameters as used by Donati et al. (2008a) namely a mass of $M_* = 0.7\,\mathrm{M}_\odot$, a radius of $R_* = 1.95\,\mathrm{R}_\odot$ and a rotation period of $P_{rot} = 7.6\,\mathrm{d}$. This implies an equatorial corotation radius,

$$R_{co} = \left(\frac{GM_* P_{rot}^2}{4\pi^2}\right)^{1/3}, \tag{1}$$

of $7.4\,R_*$. We assume a mass accretion rate of $2.88 \times 10^{-8}\,\mathrm{M}_\odot\mathrm{yr}^{-1}$ (Gullbring et al. 1998).

For V2129 Oph we adopt the same stellar parameters as used by Donati et al. (2007) and Jardine, Gregory & Donati (2008), namely a mass of $M_* = 1.35\,\mathrm{M}_\odot$, a radius of $R_* = 2.4\,\mathrm{R}_\odot$ and a rotation period of $P_{rot} = 6.53\,\mathrm{d}$. This implies an equatorial corotation radius of $R_{co} = 6.7\,R_*$. There are few estimates of the mass accretion rate on to V2129 Oph available in the literature. Eisner et al. (2005), who refer to V2129 Oph as AS 207A, estimate an accretion rate of $3.2 \times 10^{-8}\,\mathrm{M}_\odot\mathrm{yr}^{-1}$, whereas Donati et al. (2007) calculate a value of $4 \times 10^{-9}\,\mathrm{M}_\odot\mathrm{yr}^{-1}$ using the empirical relationship between accretion rate and the flux in the CaII 8662Å line presented by Mohanty, Jayawardhana & Basri (2005). We therefore assume that the disc mass accretion rate of V2129 Oph is $\dot{M} = 10^{-8}\,\mathrm{M}_\odot\mathrm{yr}^{-1}$, a compromise between both observationally inferred values.

2.2 Magnetic field measurements

From Zeeman-Doppler imaging of V2129 Oph, Donati et al. (2007) detected clear circular polarisation signals in both photospheric absorption, and accretion related emission, line profiles. The temporal variations of the Zeeman signatures was dominated by rotational modulation. In deriving a surface magnetogram it is possible to determine how the magnetic energy is distributed between the different field modes of a complex multi-polar field. In other words it is possible to determine how strong the dipole component is relative to the quadrupole component, or the octupole component, or the hexadecapole component etc. In the case of V2129 Oph the field is dominated by a 1.2 kG octupole, tilted at ∼20°with respect to the stellar rotation axis. The dipole component was found to be weak, with a polar strength of only 0.35 kG and tilted at ∼30°(Donati et al. 2007). The surface field in the visible hemisphere of V2129 Oph is dominated by a 2 kG positive radial field spot at high latitude, with the footpoints of the accretion funnel rooted in this region, but differs significantly from a dipole (Donati et al. 2007). We note that due to the limited resolution achievable by Zeeman-Doppler imaging studies, derived surface magnetograms likely miss the smallest scale field at the stellar surface. The integrated affects of many flares due to magnetic reconnection events within such small scale field regions, is likely responsible for the "quiescent" level of X-ray of emission detected from T Tauri stars (Getman et al. 2008a).

Several authors have reported the detection of magnetic fields on BP Tau (Johns-Krull, Valenti & Koresko 1999b; Johns-Krull 2007; Donati et al. 2008a) with a strong circular polarisation signal commonly detected in the accretion related HeI 5876Å emission line (Johns-Krull et al. 1999a; Valenti & Johns-Krull 2004; Symington et al. 2005; Chuntonov et al. 2007), as well as in other accretion

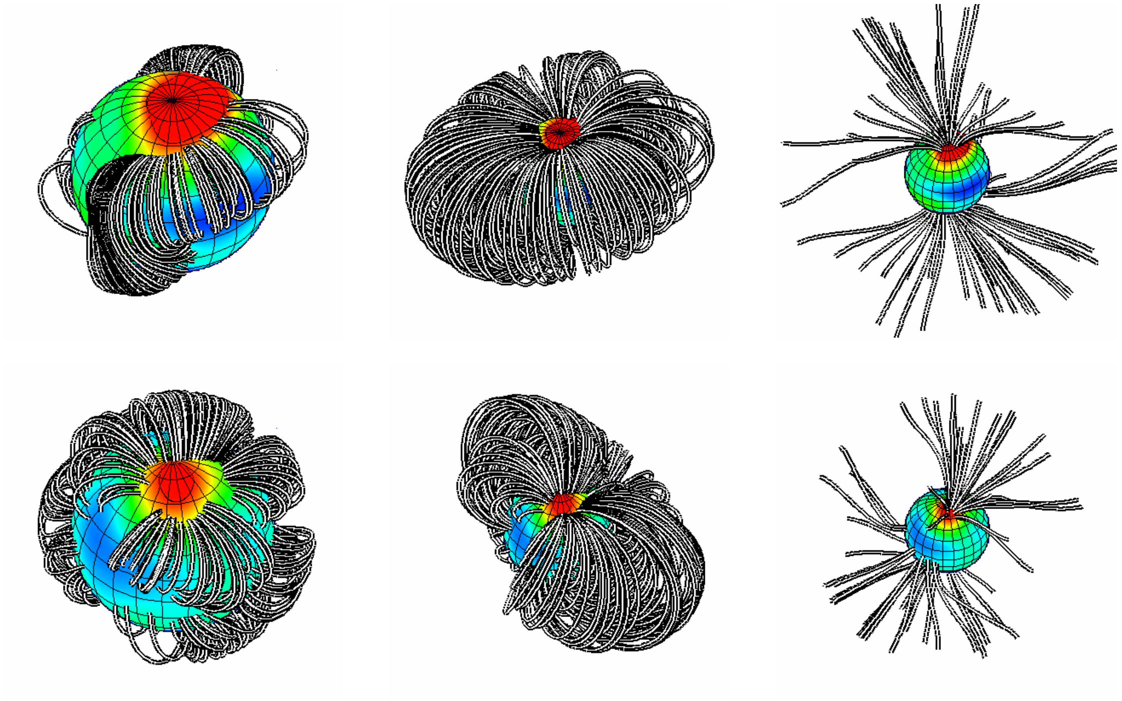

Figure 1. Field extrapolations from observationally derived surface magnetograms of BP Tau (top row) and V2129 Oph (bottom row). The left-hand panel shows the complex surface field, the middle panel the more well-ordered larger scale field, and the right-hand panel the open field lines. The stellar surface is coloured to show the polarity of the radial field component with red (blue) depicting positive (negative) field regions. The images are not to scale.

related emission lines (e.g. the CaII IRT and HeI 6678Å; Donati et al. 2008a). Despite the concerns of Chuntonov et al. (2007)[1], Donati et al. (2008a) have presented clear evidence that the Zeeman signatures in both photospheric and accretion related lines are dominated by rotational modulation, having monitored BP Tau for a complete rotation cycle at two different epochs. Interesting the large scale structure of BP Tau's field was found to be similar despite the observing runs being separated by almost 11 months. However, the magnetic features appear to have undergone an apparent phase shift of a quarter of a rotation phase, which was most likely caused by a small error in the adopted stellar rotation period (Donati et al. 2008a).[2] Although BP Tau's magnetic field is found to be complex, it is simpler than that of V2129 Oph. The field of BP Tau consists of both a strong dipole component, which at 1.2 kG is four times as strong as that of V2129 Oph, and a strong octupole component of 1.6 kG. Both the octupole and dipole moments are tilted by ∼10°with respect to the stellar rotation axis, but in different planes (Donati et al. 2008a).

3 FIELD EXTRAPOLATION

A variety of field extrapolation techniques have been developed which allow the extrapolation of coronal magnetic fields from observationally derived surface magnetograms. From the derived maps of the photospheric fields of V2129 Oph and BP Tau, we extrapolate their three-dimensional coronal field topologies using the potential field source surface model. A potential field is one which is current-free, and has the advantages over a full MHD model of faster computation speed and simplicity, and does not require an assumption about an equation of state. The disadvantages of such a model, however, are that time-dependent and non-potential effects cannot be reproduced, and these may be important when considering the interaction between the stellar field and the disc. Riley et al. (2006) provide a comparison of the two techniques, as applied to the Sun, and find that often the potential field model produces results that closely match MHD models, with Liu & Lin (2007) coming to the same conclusion for the case of stable solar active regions. For cTTSs however, the main source of non-potentiality in the field is likely to be caused by the interaction between the stellar magnetosphere and the disc, which cannot be modelled with the static field structures considered here.

---

[1] Some authors have argued that variations in the longitudinal (line-of-sight) field component, derived from polarisation detections in the HeI 5876Å line, were attributable to rotational modulation (e.g. Valenti, Johns–Krull & Hatzes 2003; Valenti & Johns-Krull 2004). Chuntonov et al. (2007) refutes such suggestions and argues that the field in the HeI 5876Å line formation region is constantly evolving and restructuring on a timescale of only a few hours. The ESPaDOnS/NARVAL spectropolarimetric data presented by Donati et al. (2008a), however, clearly show that although the HeI 5876Å line is subject to intrinsic variability, its temporal evolution is dominated by rotational modulation. This suggests the magnetic field in the HeI line formation region remains stable on timescales of longer than a rotation cycle.

[2] Due to the similarity of the derived surface magnetograms we only use the one derived from the Donati et al. (2008a) February 2006 data in this paper.

Alternative field extrapolation techniques from Zeeman-Doppler images have been considered by Hussain et al. (2002), who compared the difference between a non-potential current carrying magnetic field model, and the potential field model. By considering field extrapolations from a magnetogram of the young rapid-rotator AB Dor, they found that the ratio of free energy in the potential to that in the non-potential model differed by up to 20% close to the stellar surface. However, this difference decayed rapidly with height above the star, with only 1% difference at $1R_*$ above the photosphere, indicating little difference in the field structures derived from the potential and non-potential field models. The potential field source surface model should therefore be adequate to allow us to address the question of whether the surface magnetograms of V2129 Oph and BP Tau are consistent with the observed locations of accretion funnels and accretion hotspots, as well as to compare the large scale field topologies with that of a simple dipole.

As we have assumed that the field is potential then $\nabla \times \boldsymbol{B} = 0$. This condition can be satisfied by writing the field in terms of a scalar flux function Ψ

$$\boldsymbol{B} = -\nabla\Psi. \tag{2}$$

The field must also satisfy Maxwell's equation, $\nabla \cdot \boldsymbol{B} = 0$, and therefore Ψ must satisfy Laplace's equation, $\nabla^2\Psi = 0$. This has a standard solution of the form,

$$\Psi = \sum_{l=1}^{N} \sum_{m=-l}^{l} \left[a_{lm} r^l + b_{lm} r^{-(l+1)} \right] P_{lm}(\theta) \mathrm{e}^{im\phi}, \tag{3}$$

where P_{lm} denote the associated Legendre functions and the coefficients a_{lm} and b_{lm} are determined from the boundary conditions. The first boundary condition is that the strength of the radial component of the field at the stellar surface is that which is derived from the Zeeman-Doppler maps of the star. The second condition is that at some height above the stellar surface R_S, known as the *source surface*, the field becomes radial and hence $B_\theta(R_S) = B_\phi(R_S) = 0$, emulating the effect of the corona blowing open field lines to form a stellar wind (Altschuler & Newkirk 1969). Thus, from (2) it is possible to determine the magnetic field components, B_r, B_θ, and B_ϕ, and therefore a field vector, at any point within the stars corona (see Gregory et al. (2006a) for the full expressions). In order to extrapolate the field we used a modified version of a code originally developed by van Ballegooijen, Cartledge & Priest (1998), and applied specifically to T Tauri stars by Jardine et al. (2006) and Gregory et al. (2006a,b, 2007).

The field extrapolations showing the smaller scale, larger scale, and open field structure of V2129 Oph and BP Tau, are shown in Fig. 1. For both stars we have set the source surface to be at the corotation radius (see §2.1), which at this stage serves only to illustrate the difference between the complex and loopy surface field regions, and the well-ordered larger scale field. Later we discuss how variations in the source surface radius affects the structure of the field. It is clear from Fig. 1 that for both stars the largest scale field resembles a slightly tilted dipole, especially in the case BP Tau. But how does the larger scale field extrapolated from observationally derived surface magnetograms, compare to a simple dipole magnetic field?

3.1 Comparison with a large scale dipole field

The complex field structures obtained by field extrapolation of both V2129 Oph, and in particular BP Tau, appear to indicate that the larger scale field is well ordered, and much simpler than the loopy and compact surface field regions. In this section we compare the larger scale field topology with that of a modified dipolar field. Taking the $l = 1$, $m = 0$ component of equation (3) and imposing the boundary conditions

$$\begin{aligned} B_r(R_*) &= \frac{2\mu}{R_*^3}\cos\theta && (4)\\ B_\theta(R_S) &= B_\phi(R_S) = 0, && (5) \end{aligned}$$

allows the construction of a dipole field with a source surface, where $\mu = R_*^3 B_{*,pole}/2$ is the dipole moment and $B_{*,pole}$ the polar strength of the dipole. The inclusion of a source surface introduces a modification to the standard dipole field components,

$$\begin{aligned} B_r &= \frac{2\mu\cos\theta}{r^3}\left(\frac{r^3 + 2R_S^3}{R_*^3 + 2R_S^3}\right) && (6)\\ B_\theta &= \frac{\mu\sin\theta}{r^3}\left(\frac{-2r^3 + 2R_S^3}{R_*^3 + 2R_S^3}\right) && (7)\\ B_\phi &= 0, && (8) \end{aligned}$$

which are recovered in the limit of $R_S \to \infty$. Individual field lines can be described by,

$$\sin^2\theta = \frac{\xi r}{r^3 + 2R_S^3}, \tag{9}$$

where ξ is a constant along a particular field line, such that different values of ξ correspond to different field lines. The last closed field line passes through the stars equatorial plane ($\theta = \pi/2$) at $r = r_m = R_S$, and therefore $\xi = 3R_S^2$. Such a field line connects to the stellar surface at a co-latitude of θ_m where

$$\theta_m = \sin^{-1}\left(\sqrt{\frac{3R_S^2 R_*}{R_*^3 + 2R_S^3}}\right). \tag{10}$$

The structure of such a modified dipolar field is illustrated in fig. 1 of Jardine et al. (2006). We note that the dipole components of the fields of both BP Tau and V2129 Oph are slightly tilted with respect to the stellar rotation axis (10°for BP Tau and 30°for V2129 Oph). We account for this small tilt below when comparing the complex field structures to that of the dipolar fields. Mahdavi & Kenyon (1998) provide analytic expressions for calculating the components of an arbitrarily tilted dipole, which we adapt in order to include the source surface, and calculate the tilted dipole field components numerically using our field extrapolation code.

The black points in Figs. 2 and 3 show field line length against width calculated from the field extrapolations of the magnetic fields of BP Tau and V2129 Oph, for source surface radii of $R_S = 2.5\,R_*$ and $R_S \approx R_{co}$. At this stage such plots are used only to illustrate by how much the field structure departs from a simple dipole (red points in Figs. 2 and 3). We define the length of a field line as being the radial distance measured from the stellar surface to the maximum height

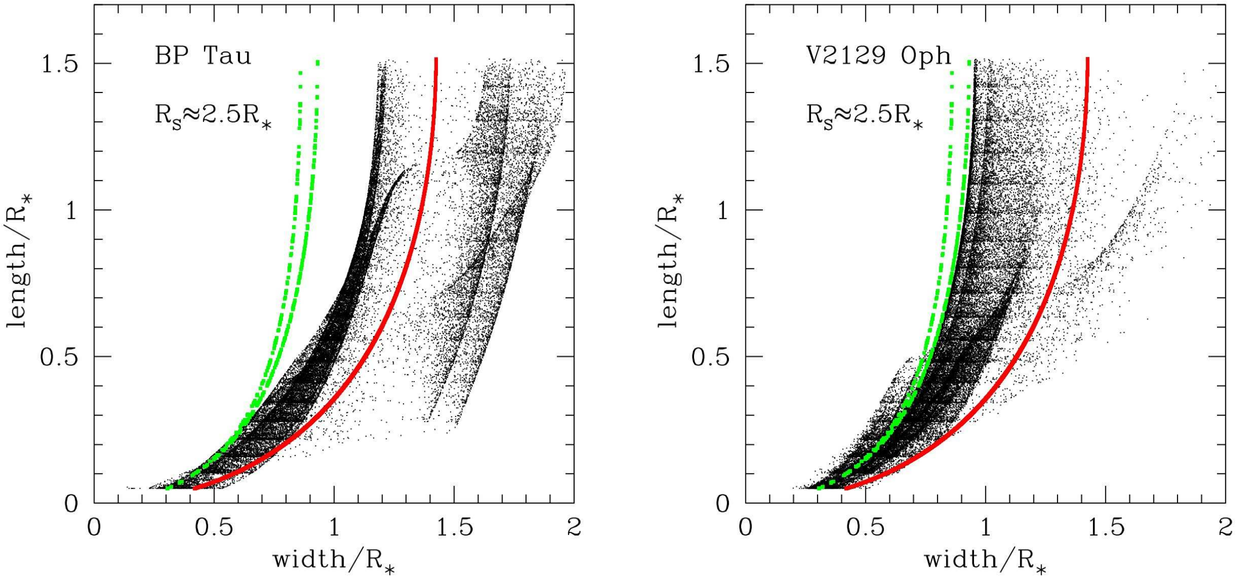

Figure 2. Plots of field line length (maximum radial distance above the stellar surface) against field line width (the distance along a segment of the great circle connecting the field line footpoints on the stellar surface) for BP Tau (left panel) and V2129 Oph (right panel). A source surface radius of $2.5\,R_*$ has been assumed. The black points are for the extrapolated fields, the red points indicate the behaviour of a dipole field, and the green points an octupole field.

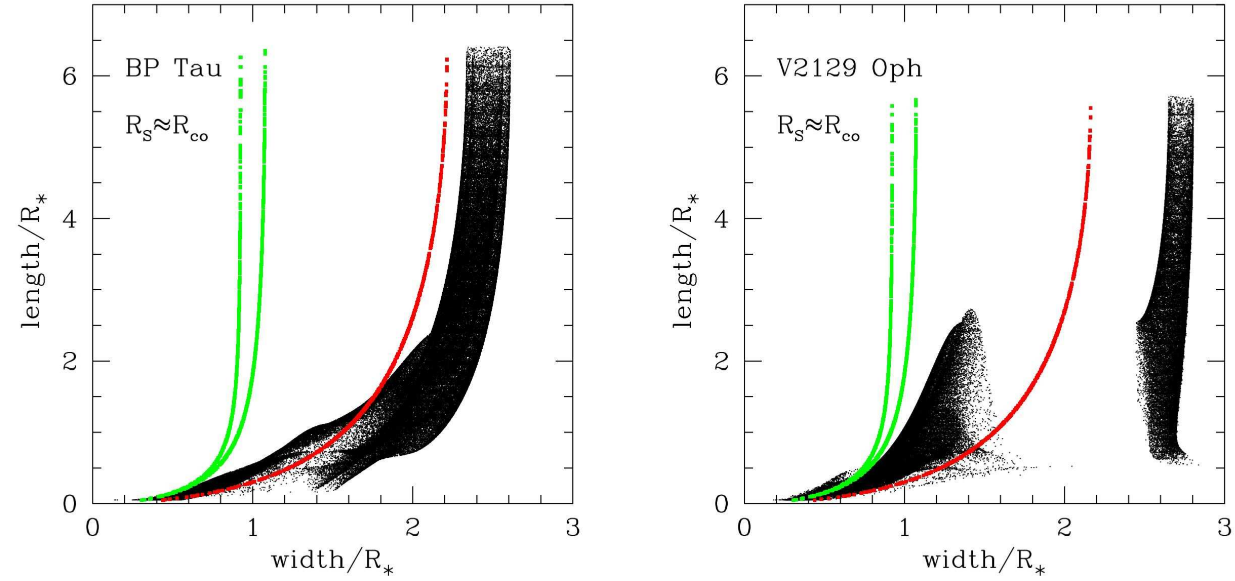

Figure 3. The same as Fig. 2, but assuming that the source surface is at approximately the corotation radius, which is $7.4\,R_*$ for BP Tau (left panel) and $6.7\,R_*$ for V2129 Oph (right panel).

of the field line. The width of a field line is defined as the distance along the segment of the great circle connecting the field line footpoints on the stellar surface. For a field line with footpoints at *co-latitudes* and longitudes (θ_1, ϕ_1) and (θ_2, ϕ_2) the width, w, can be calculated using the Haversine formula,

$$h = \sin^2\left(\frac{\Delta\theta}{2}\right) + \sin\theta_1 \sin\theta_2 \sin^2\left(\frac{\Delta\phi}{2}\right) \qquad (11)$$

$$w = 2\sin^{-1}\left(\sqrt{h}\right), \qquad (12)$$

where $\Delta\phi = \phi_2 - \phi_1$ is the longitudinal separation between the footpoints, $\Delta\theta = |\theta_2 - \theta_1|$ is the difference in co-latitudes, and where all angles are measured in radians and all distances in units of stellar radii.

By considering progressively longer field line loops, Figs. 2 and 3 show that for a dipole field the field line width eventually tends asymptotically to a certain value which depends on the choice of source surface. This is as expected, as by equation (10) the co-latitude of the footpoint of the longest dipole field line depends on the choice of source surface R_S, with θ_m being smaller for a larger R_S (and for an aligned dipole field line the latitudinal footpoint separation is $\Delta\theta = \pi - 2\theta_m$ radians). We also show in Figs. 2 and 3 the behaviour of an octupole magnetic field (green points). For an axial octupole ($l = 3, m = 0$) the width of the closed field line loops about the stellar equator is less than those at higher latitudes (see the discussion in Willis & Young 1987), which gives rise to two separate lines in the length vs width plots.

For a small source surface (see Fig. 2) the longer field lines on BP Tau are typically wider than those on V2129 Oph. This reflects the strength of the dipole components in the two stars, which is about 4-times stronger on BP Tau than V2129 Oph (stars with a strong dipolar field component would typically have wider field lines, connecting the different polarity poles in opposite hemispheres), and also the dominantly octupolar nature of V2129 Oph's field. In both cases, however, the fields are more complex than a dipole. For the case of a large source surface (see Fig. 3) the field structure of BP Tau follows a similar trend to the dipole field, as do the longest field lines on V2129 Oph. However, many of the smaller scale field lines on V2129 Oph are not as wide as the dipolar field lines. This suggests that the smaller scale field on V2129 Oph is complex and multi-polar with the field strength decaying more rapidly with height than on BP Tau; we return to this point in §5. For V2129 Oph the smaller scale field (see Fig. 2) is more closely matched to an octupole field. Also, some of the shortest width field lines are longer than those of an octupole, indicating a contribution to the surface field from the higher order field modes. Indeed, for V2129 Oph there is also a significant amount of magnetic energy in the $l = 5$ field mode (Donati et al. 2007).

The field structure of V2129 Oph is particularly striking when a large source surface is considered (Fig. 3, right panel). The surface magnetic field of V2129 Oph is dominated by large 2 kG positive radial field spot at high latitude in the visible hemisphere, and likely a similar negative field region in the unseen hemisphere (Donati et al. 2007). While the surface field region consists of many small width loops, the larger scale field comprises of the longer magnetic loops which connect to the high latitude field regions. This behaviour is not apparent when considering V2129 Oph with a smaller source surface, as the co-latitude at which the last closed field line connects to the stellar surface is larger, by equation (10), which means that field lines cannot connect to the large high latitude radial field spots. With a large source surface the longest field lines are always wider than those of a dipole, suggesting that the structure of the field lines are being affected by the strong field regions close to the stellar surface; with such field lines connecting at smaller co-latitudes than a dipole field. This effect is more apparent for V2129 Oph, where the larger scale field lines are "squeezed" by the strong dominantly octupolar field close to the stellar surface. This forces such field lines to have larger widths at a given length. This is also the case for the field of BP Tau (see Fig 3, left panel), however, the effect is less due to the strength of octupole component relative to the dipole component being over 2.5 times less for BP Tau than for V2129 Oph. The structure of the largest scale field lines therefore depart from the path followed by purely dipolar field lines. It is such larger scale loops which are likely to be carrying material from the disc to the star. Therefore the location of accretion hotspots on the stellar surface will differ from what is expected from dipolar accretion, even though the larger scale field is relatively well-ordered and similar to a dipole. In the following sections we look more closely at the structure of the open and accreting field.

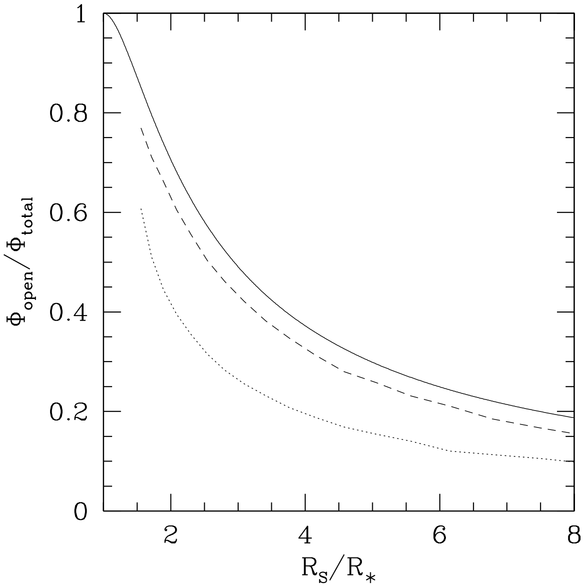

Figure 4. The variation of the ratio of open to total flux through the stellar surface for a range of source surface radii. The solid line represents the modified dipole magnetic field, the dashed line the field of BP Tau and the dotted line the field of V2129 Oph. There is less fractional open flux when considering magnetic fields with a realistic degree of complexity.

4 THE OPEN FIELD

The amount of open flux passing through the stellar surface is important for models of stellar winds, which for cTTSs may remove the angular angular momentum which would be transfered to the star due to accretion (Matt & Pudritz 2005b). It is therefore of interest to compare the amount of open flux for V2129 Oph and BP Tau with that of the modified dipole magnetic field. Since the magnetic torque in a stellar wind does not depend on the polarity of the field, we consider here the absolute value of the flux. The open flux through the stellar surface is given by

$$\Phi_{open} = R_*^2 \int\int |B_{r,open}(\theta,\phi)| d\Omega. \tag{13}$$

Using equation (4) an expression for Φ_{open} can be derived for our modified dipole field,

$$\begin{aligned}\Phi_{open} &= 2R_*^2 \int_0^{2\pi} d\phi \int_0^{\theta_m} \frac{2\mu}{R_*^3} \cos\theta \sin\theta d\theta \quad (14)\\ &= 2\pi R_*^2 B_{*,pole} \sin^2\theta_m. \quad (15)\end{aligned}$$

where the additional factor of 2 accounts for the open field in each hemisphere. A similar expression can be derived for

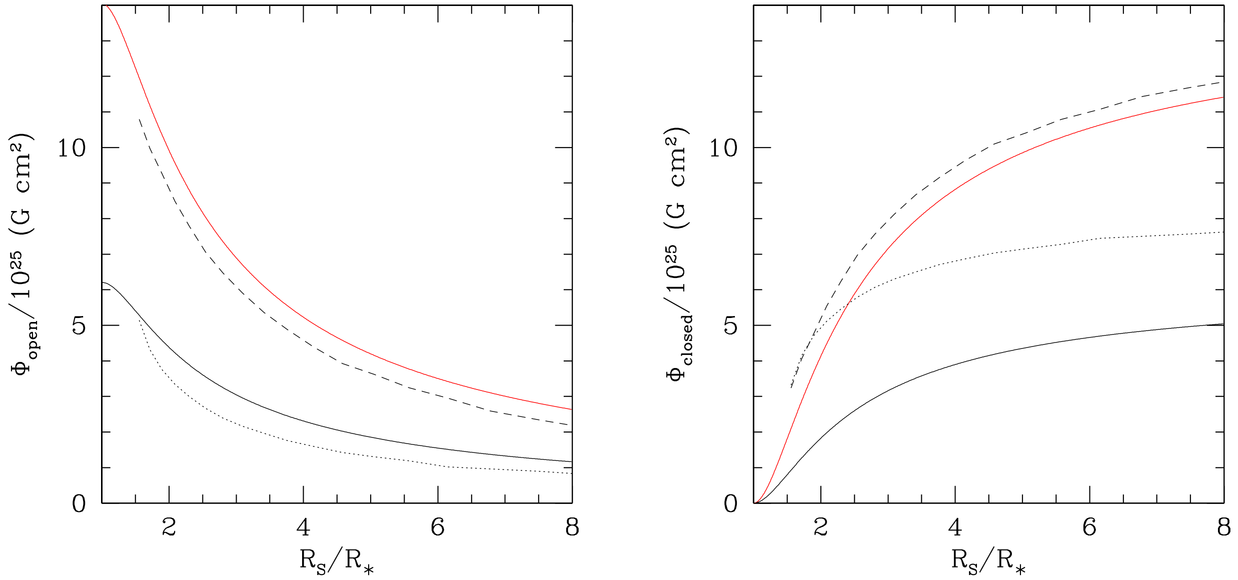

Figure 5. The variation of open and closed flux (left and right panels respectively) through the stellar surface for a range of source surface radii. The solid lines represent modified dipole magnetic fields, with the red (black) line representing a polar field strength of 1.2 (0.35) kG. The dashed line represents the field of BP Tau and the dotted line the field of V2129 Oph. There is less open flux, but more closed flux, when considering the complex magnetic fields.

the closed flux through the stellar surface,

$$\Phi_{closed} = 2R_*^2 \int_0^{2\pi} d\phi \int_{\theta_m}^{\pi/2} \frac{2\mu}{R_*^3} \cos\theta \sin\theta d\theta \quad (16)$$

$$= 2\pi R_*^2 B_{*,pole} \cos^2\theta_m. \quad (17)$$

Thus for the modified dipole field the ratio of open flux to the total flux through the stellar surface is,

$$\frac{\Phi_{open}}{\Phi_{total}} = \sin^2\theta_m = \frac{3R_S^2 R_*}{R_*^3 + 2R_S^3}, \quad (18)$$

where the total flux $\Phi_{total} = \Phi_{open} + \Phi_{closed}$. The solid line in Fig. 4 shows the variation of the fractional open flux Φ_{open}/Φ_{total} for a range of different source surface radii R_S assuming a modified dipolar magnetic field. For large source surface radii the colatitude of the footpoint of the last closed field line is close to the pole of the star, and therefore the open flux through the stellar surface is less. As the source surface radius is decreased more of the closed field is converted to open field along which a (stellar) wind may be launched.

For the magnetic fields extrapolated from the surface magnetograms we divide the stellar surface into a series of small grid cells. Within each grid cell we take the average of the magnitude of B_r, at the footpoint of the open field lines and multiply this by the area of the cell in order to calculate the open flux from that individual cell. If a cell contains the footpoints of both open and closed field lines we weight the area of that cell accordingly. For example, a cell containing 50% open field, is assumed to contribute 50% of it's area to the open flux. The total open flux through the stellar surface is then obtained by summing over all the cells, while the total closed flux is calculated in a similar way. We find that there is less fractional open flux through the surface of V2129 Oph and BP Tau (dotted and dashed line in Fig. 4) compared with the dipole field. This is consistent with our argument in the previous section that the structure of the larger scale field (and in particular that of V2129 Oph) is influenced by the strong field regions closer to the star. As the larger scale field lines are wider than those of a dipole, their footpoints are closer to the pole (see Fig. 3). Thus there is less area of the stellar surface available from which a stellar wind can be launched along the open field.

The lower fractional open flux for the complex fields, can be understood by considering how the open and closed flux changes as the source surface location is varied. This is illustrated in Fig. 5, where the solid lines represent dipole magnetic fields. In order to compare the fluxes of the complex fields with a dipole, we have assumed that the dipole has a polar strength equal to that of the measured dipole components of V2129 Oph and BP Tau (0.35 kG and 1.2 kG respectively). Both stars have slightly less open flux compared to a dipole, but more closed flux. There is significantly more closed flux for V2129 Oph compared to a dipole than for BP Tau. This is simply a reflection of the more complex nature of V2129 Oph's magnetic field, and is the largest factor in explaining why the fractional open flux for this star is well below the dipole case (see Fig. 4).

The main result of this section is that there is less fractional open flux for the complex field geometries, compared to a pure dipole case. This is result of the complex fields having both lower open flux, and, in particular, higher closed flux. This is understandable since a more complex field geometry is characterised by more numerous and smaller closed magnetic loops.

5 THE ACCRETING FIELD

It has long been suspected that the magnetic fields of cTTSs are more complex than a simple dipole, with, for example, Edwards et al. (1994) arguing that the common detection of inverse P-Cygni profiles was evidence for multiple accreting loops in a field configuration more complex than a dipole. Until very recently, however, only indirect clues were available to the complex nature of T Tauri magnetic fields. The detection of rotationally modulated X-ray emission in a small, but significant, sample of T Tauri stars indicated that X-ray emitting plasma was confined to compact field regions in-homogeneously distributed about the stellar surface (Flaccomio et al. 2005). Such modulated X-ray emission would not occur if the surface field was dipolar. Further clues to the complex nature of T Tauri surface fields comes from the common failure to detect polarisation signals in photospheric absorption lines, despite strong average fields being measured from the Zeeman broadened, and unpolarised, intensity spectra (Valenti & Johns-Krull 2004). This suggested that the surface of T Tauri stars were covered in many regions of opposite polarity. Spectral lines forming in such magnetic regions would be polarised in the opposite sense, leading to a cancellation of the polarisation signal along the line-of-sight to the observer. However, often a strong polarisation signal is detected in accretion related emission lines (e.g. Johns-Krull et al. 1999a) which is modulated due to the stellar rotation (Valenti & Johns-Krull 2004). This suggests that such emission lines are forming in regions of the stellar atmosphere which are permeated by field lines of a single magnetic polarity which remains stable as the star rotates. In other words, despite the clues to the complex nature of T Tauri surface fields, the accreting field lines are likely anchored in single polarity regions, and the field connecting to such regions may be well-ordered and more like a dipole.

The resolution achievable with ESPaDOnS (and its twin instrument NARVAL) has allowed the detection of polarisation signals in both photospheric absorption, and accretion related emission, lines, and has confirmed the complex nature of magnetic fields of cTTSs (Donati et al. 2007, 2008a). However, magnetospheric accretion models developed thus-far have yet to account for the true complexity of the stellar magnetic field. The first steps in considering how realistic multi-polar fields would influence accretion from the inner disc were taken by Gregory et al. (2005, 2006a) and Jardine et al. (2006). More recently the 3D MHD simulations of Long et al. (2007, 2008) have considered a quadrupole-dipole composite field. However, simulations incorporating generalised multi-polar magnetic fields are now required, and will shed new-light on the star-disc interaction.

For the stars where magnetic surface maps have been obtained to date the bulk of accretion in the visible hemisphere is channelled into a single magnetic spot at high latitude (Donati et al. 2007, 2008a). In order to explain the location of high latitude hotspots, the source surface has to be large enough to allow field lines to connect between the high latitude radial field spots close to the poles. The source surface radius represents the extent of the closed stellar magnetosphere and independently obtained observations provide justification for setting the source surface to be at least equal to the corotation radius. Getman et al. (2008a,b) have analysed flares detected during the *Chandra* Orion Ultradeep Project, using a new technique that allows the modelling of flaring events which are much fainter than those accessible by traditional parametric flare modelling techniques (e.g. Favata et al. 2005). By calculating the lengths of the magnetic loops containing the flares, Getman et al. (2008b) have found evidence for magnetic structures that extend well beyond the corotation radius radius in weak-line T Tauri stars, however for classical T Tauri stars the magnetic loops are all confined to within the corotation radius. This suggests the presence of a disc is limiting the extent of the closed stellar magnetosphere of accreting T Tauri stars - as previously predicted by Jardine et al. (2006). The Getman et al. (2008b) results therefore provide strong evidence that the stellar magnetosphere in classical T Tauri stars never extends to beyond the corotation radius, suggesting that setting the source surface to be at corotation is a reasonable assumption. However, the location of the disc truncation radius may still be closer to the stellar surface. With a large source surface field lines are able to connect to the high latitude field regions, even well within the corotation radius. Thus if the disc is truncated at, or even within, the corotation radius, then accretion may proceed along field lines which connect to a high enough latitude in order to explain the observed hotspot locations. Therefore an interesting question to ask is how would the disc truncation radius differ between dipole and more complex magnetic field models?

5.1 The inner disc radius

The question of where the disc is truncated, and therefore the structure of the magnetic field threading the disc and carrying accreting gas, remains a major problem for accretion models. It is still unknown if the disc is truncated in the vicinity of the corotation radius, the assumption of traditional accretion models (e.g. Königl 1991), or whether it extends closer to the stellar surface (e.g. Matt & Pudritz 2005b). As in Gregory et al. (2007) we assume that accretion occurs over a range of radii within the corotation radius. This is equivalent to the approach taken previously by Hartmann, Hewett & Calvet (1994), Muzerolle, Calvet & Hartmann (2001), Symington et al. (2005), Azevedo et al. (2006) and Kurosawa, Harries & Symington (2006) who have demonstrated that such an assumption broadly reproduces observed spectral line profiles and variability. It should also be noted that the accreting field geometries which we consider here are only snap-shots in time, and in reality will evolve due to the interaction with the disc.

Bessolaz et al. (2008) provide an overview of the various assumptions that have been used in the literature to calculate the disc truncation radius. Here we provide rough estimates of the inner disc radius for BP Tau and V2129 Oph based on their extrapolated magnetic fields, and compare these values with those calculated by assuming both stars have dipole magnetic fields.

We assume that the location of the inner disc is the radius at which the torque due to viscous processes in the disc is comparable to the magnetic torque due to the stellar magnetosphere. This is equivalent to the approach taken previously by several authors, for example, Clarke et al. (1995) and Wang (1996). This torque depends on how much the disc is able to twist the field lines of the stellar magnetosphere.

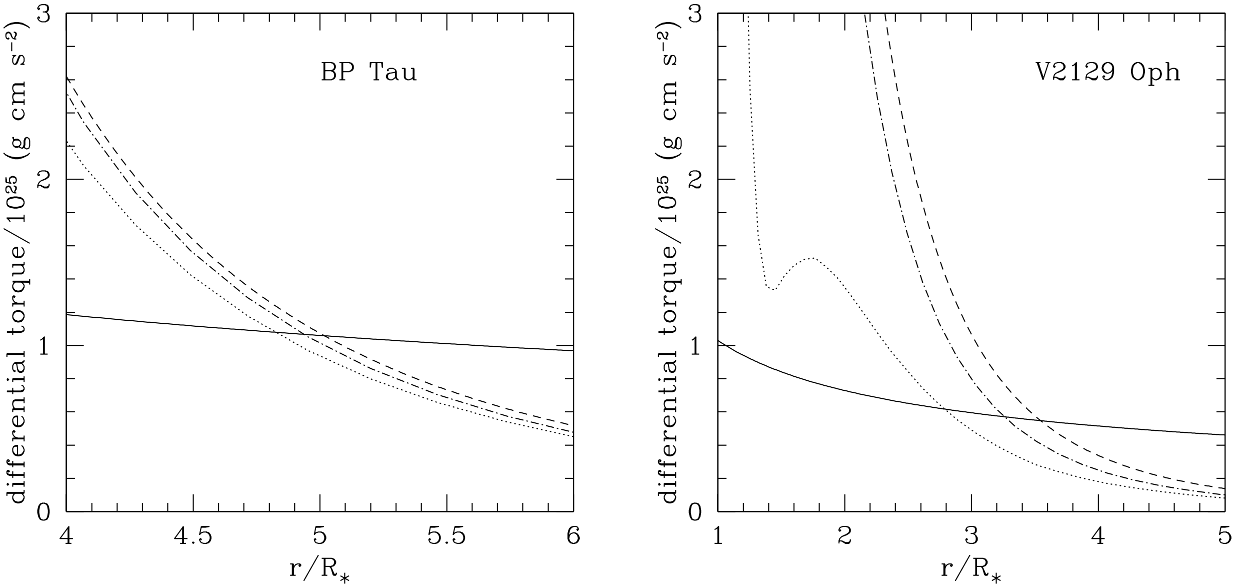

Figure 6. The variation along the equatorial plane of the differential magnetic/viscous torque [i.e. the LHS and RHS of equation (19)] for BP Tau (left panel) and V2129 Oph (right panel). The solid line represents the RHS of (19), with the LHS for an aligned dipole field (dashed line), a tilted dipole field with a source surface (dash-dot line) and the field extrapolation of V2129 Oph/BP Tau (dotted line). In both cases the disc is truncated well within the corotation radius of $6.7\,R_*$ (V2129 Oph) and $7.4\,R_*$ (BP Tau), although the exact location of R_t is very sensitive to the assumed accretion rate.

We approximate that this twist at the location of the inner disc is of order 45°i.e. at the inner disc we assume that the perturbed toroidal component is equal to the poloidal component ($B_\phi \sim B_z$). This assumption should be valid as long as the disc is truncated sufficiently within the corotation radius and assuming the disc is strongly coupled to the stellar magnetic field (Matt & Pudritz 2005a). Equating the differential magnetic and viscous torques, and assuming that the poloidal field threading the disc is dominated by the vertical component ($B_z \gg B_r$), gives

$$r^2 B_z^2 = \frac{1}{2}\dot{M}\left(\frac{GM_*}{r}\right)^{1/2}. \qquad (19)$$

Note that this equation assumes a cylindrical corordinate system, however as we are restricting the problem to the star's equatorial plane, the cylindrical radius and the spherical radius are the same, and $B_z = B_\theta$. Interestingly, the disc disruption radius found in the numerical simulations of Long et al. (2005) (see the discussion in their section 2) approximately conincides with that derived through the use of equation (19). The solid line in Fig. 6 represents the variation in the RHS of this equation along the stars equatorial plane, using the stellar parameters given in §2.1. The various dashed and dotted lines in Fig. 6 represent the LHS of this equation assuming different forms for the stellar magnetic field. The value of r where the lines representing the LHS and RHS of equation (19) cross, is then the disc truncation radius R_t.

For a dipole magnetic field the variation in B_z along the equatorial plane can be written as

$$B_z = B_\theta = \frac{1}{2}B_{*,pole}\left(\frac{R_*}{r}\right)^3. \qquad (20)$$

The dashed lines in Fig. 6 represent such an aligned dipole field with a polar strength of $B_{*,pole} = 1.2\,\mathrm{kG}$ for BP Tau and 0.35 kG for V2129 Oph, i.e. dipole fields with the same polar strength as the dipole components of the measured fields of both stars (see §2.2). With such an assumption for the stellar magnetic fields, we obtain a disc truncation radius of $\sim 5R_*$ for BP Tau and $\sim 3.6R_*$ for V2129 Oph. This is well within the corotation radius in both cases, justifying our assumption that the perturbed toroidal component of the field equals the poliodal component at the inner edge of the disc ($R_t \sim 0.7R_{co}$ for BP Tau and $R_t \sim 0.5R_{co}$ for V2129 Oph). However, for a better comparison with the extrapolated fields we consider modified and tilted dipole fields, i.e. dipole fields with a source surface, tilted by the same amount as the dipole component in both stars. Once the dipole field been tilted, the magnetic field is no longer axisymmetric in the stars equatorial plane, and therefore B_z is no longer uniform in azimuth at a fixed radius. At each radius r we therefore take the average of the square of B_z for use in equation (19)[3] (note that we follow the same procedure for the extrapolated fields discussed below). The dash-dot lines in Fig. 6 represent such tilted dipoles, with the disc truncation radius being slightly closer to the stellar surface for such fields due to the non-uniformity of B_z in azimuth. In Fig. 6 (and Figs. 8 and 7 below) we have chosen to set $R_S = 20\,R_*$ in order to minimise the effects of the source surface boundary condition upon the field structure close to the accreting field regions.

We have already seen in §3.1 that the larger scale field of BP Tau is similar to a dipole, but that the field of V2129 Oph shows significant departures from such a simple field configuration. We therefore expect that the disc truncation radius calculated using the extrapolated field of BP Tau will be similar to that of a dipole while R_t for V2129 Oph may be different. The dotted lines in Fig. 6 demonstrate that this is indeed the case, with R_t for BP Tau closely matched to that of the modified dipole. This is due to the strong dipole component of BP Tau's field, which contains 50% of the magnetic energy (Donati et al. 2008a), and is 4-times stronger than the dipole component of V2129 Oph. The calculated inner disc radius for V2129 Oph is closer to the stellar surface than would be expected for a dipole field. This is a reflection of the intrinsic field complexity of V2129 Oph, and the rapid drop off in field strength with height above the stellar surface for its magnetic field (see §5.2 below). When the magnetic field of the central star is particularly complex, as in the case of V2129 Oph, we find that the inner disc is truncated closer to the stellar surface than would be expected from dipole magnetic field models. However, the use of equations such as (19) in calculating disc truncation radii for individual stars should be treated with caution. Firstly, the values of R_t determined here are very sensitive to the assumed mass accretion rates $\dot{M}$, which are poorly constrained observationally. For example, only a factor of 2 difference in our assumed accretion rate for BP Tau of $2.88 \times 10^{-8}\,\mathrm{M}_{\odot}\mathrm{yr}^{-1}$ would change the inner disc radius from $4.8R_*$ to $3.9R_*$ or $5.9R_*$ depending on whether the accretion rate is increased or decreased respectively. Secondly, equation (19) assumes that the field threading the disc is dominated by the vertical component B_z, and although this is the case for the dipole-like large scale field of BP Tau, it is not true for V2129 Oph where the field has a significant radial component at the stellar equatorial plane. Thus the shear within the disc of V2129 Oph may generate a significant toroidal component, invalidating the use of equation (19), and suggesting that our qualitative calculation of the disc truncation radius is too simplistic. An MHD simulation using the extrapolated fields as starting points would be welcome here, in order to calculate inner disc radii more quantitatively. However, our conclusion that the inner disc should be truncated at, or within, the location obtained when considered a dipole magnetic field should remain valid.

---

[3] Once the dipole has been tilted the field threading the disc has a small radial component, however for small dipole tilts this remains much smaller than B_z.

5.2 Structure of the accreting field

In the previous sections we compared the structure of the magnetic fields of V2129 Oph and BP Tau to that of a dipole. In this section we select out only those field lines which would be able to interact with the accretion disc and carry material on to the star. In order to select such field lines we follow the algorithm discussed by Gregory et al. (2006a, 2007), which we only summarise here.

We consider a thin accretion disc and for V2129 Oph assume that the disc normal is parallel to the stellar rotation axis, such that the disc mid-plane is aligned with the stars equatorial plane. By extrapolating the field of BP Tau, Donati et al. (2008a) argued that a flat disc model could not explain the observed location of accretion hotspots. For material to accrete into the observed hotspot locations, either the disc must be tilted relative to the stellar rotation axis (i.e. aligned with the stellar magnetic equator - similar to the scenario found during the 3D MHD simulations of Romanova et al. 2003), or the inner disc must be warped. Radio CO maps of BP Tau's disc suggest a disc inclination of 30°offset from the stellar inclination of 45°(Simon, Dutrey & Guilloteau 2000), although both values are rather uncertain. Analytic arguments suggest that a large scale tilted magnetosphere (as possessed by BP Tau) will warp the inner disc, allowing material to accrete on to latitudes which are inaccessible if accretion were to proceed from a flat, wedge-shaped, disc (Terquem & Papaloizou 2000). Furthermore, the 3D MHD simulations of Romanova et al. (2003), suggest that complicated inner disc warps may arise due to the interaction of the magnetosphere with the disc. There is also strong evidence for the stellar field warping the disc in at least one other star, AA Tau (e.g. Bouvier et al. 2007), which is inclined such that our line-of-sight to the star looks through the inner disc. Given the smaller inclination of BP Tau ($i = 45°$), however, photometric eclipses due to a dense inner disc warp crossing our line-of-sight are not expected. For BP Tau we therefore assume that the disc is slightly tilted, or equivalently that the inner disc has been warped by the stellar magnetosphere[4]. An obvious question to ask, however, is why did Donati et al. (2007) find that a flat disc model was sufficient to explain the observed hotspot locations on V2129 Oph, but Donati et al. (2008a) find that a small inner disc warp was required for BP Tau? This is likely related to the strength of the dipole component on both stars, which is almost 4-times stronger on BP Tau than V2129 Oph. At the inner disc, at a distance of a few stellar radii, the dipole component is likely dominant, with the strength of the higher order field components dropping faster with height above the star. The larger scale magnetosphere of BP Tau is therefore more likely to distort the circumstellar disc. Indeed to explain the hotspot locations on BP Tau the disc had to be tilted in the same direction as the dipole moment. Tilting the disc in a similar way for V2129 Oph makes little difference to the hotspot location, suggesting that it is the strength of the dipole that is affecting the inner disc. Further numerical simulations of how magnetic fields with a realistically complexity can distort the structure of the disc will be required in future to confirm this, and are currently being undertaken.

In order to compare the structure of the complex fields of V2129 Oph and BP Tau with that of a dipole we consider how fast the field strength drops with height above the stellar surface. We therefore compare how the ratio $B(r)/B_*$ varies with r, where $B(r)$ is the strength of the field at some position r along the path of a field line and B_* the field strength at the field line footpoint. r is the spherical radius measured from the centre of the star. Figs. 7 and 8 show such plots for both V2129 Oph and BP Tau. All $B(r)/B_*$ values are plotted from the disc mid-plane to the field line footpoint at the stellar surface. Accretion is assumed to occur along all field lines threading the mid-plane of the disc across a range of radii. In Fig. 7 we assume that accretion is occuring from the corotation radius, down to $0.75\,R_{co}$ ($\sim 5 - 6.7\,R_*$ for V2129 Oph and $\sim 5.5 - 7.4\,R_*$ for BP Tau), whereas in Fig. 8 we assume that accretion is occuring from a range of

---

[4] We note, however, that the differences in the accreting field structure shown in Figs. 8 and 7 for BP Tau are almost negligible when considering a flat or slightly warped disc.

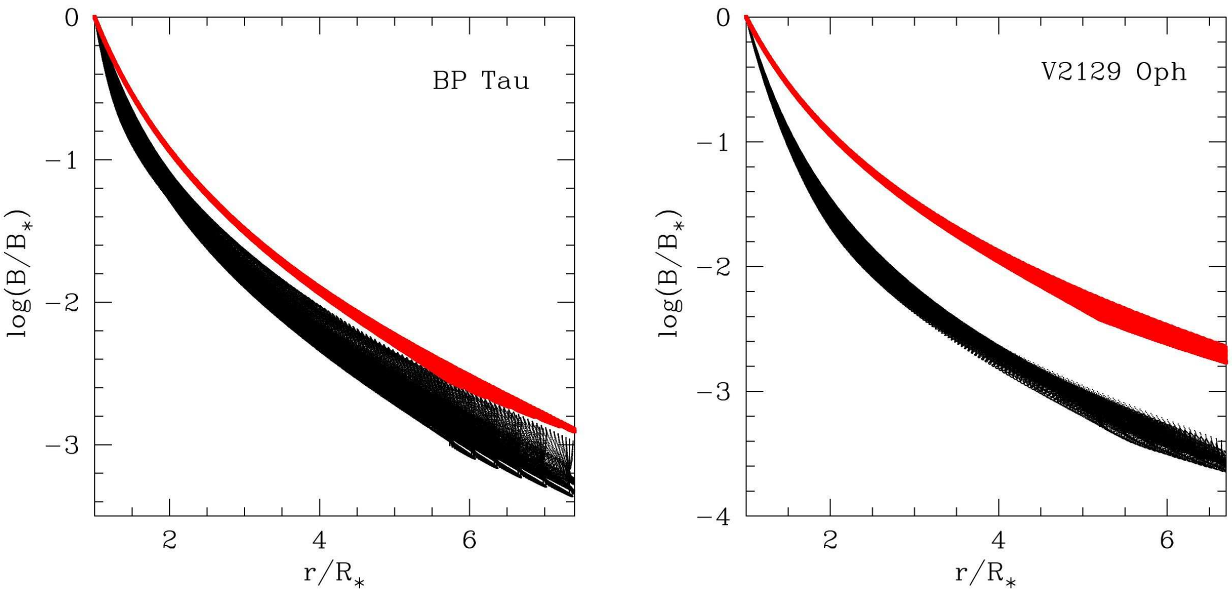

Figure 7. The drop in field strength with height above the surface of BP Tau (left panel) and V2129 Oph (right panel) along the accreting field lines (black points). Also shown for comparison is a dipole field (red points). The dipole has been tilted by 10°(30°) for comparison with the field of BP Tau (V2129 Oph). Accretion is assumed to occur from the corotation radius to $\sim 0.75\,R_{co}$.

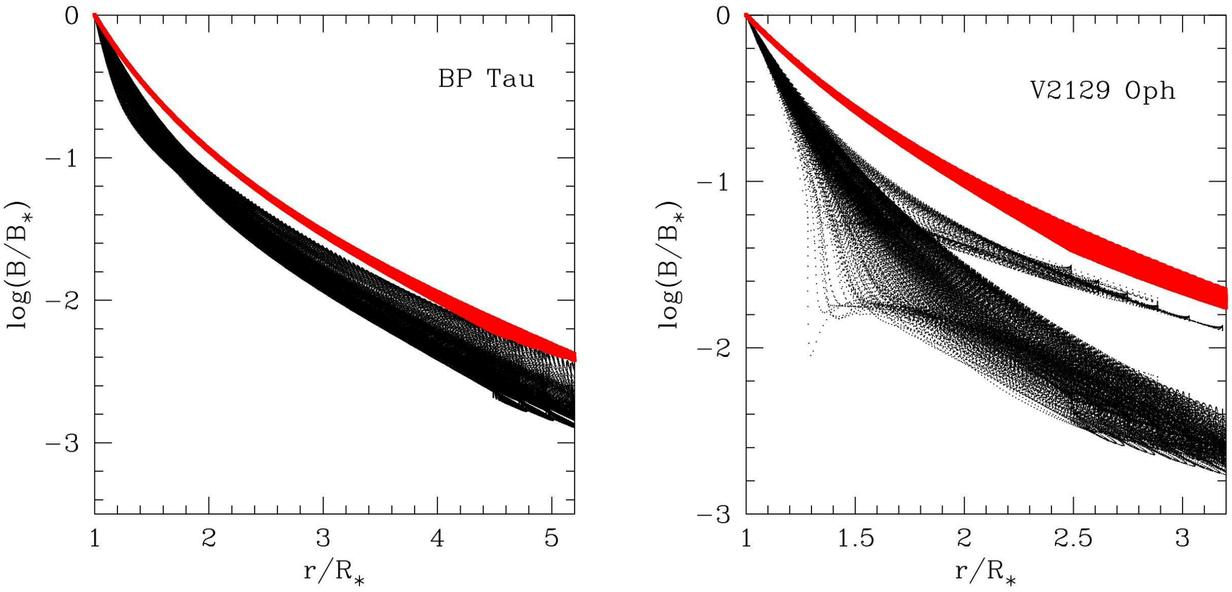

Figure 8. The same as Fig. 7, but assuming that accretion is occuring from a range of radii about the disc truncation radius, as calculated in §5.1 (see Fig. 6). The structure of the accreting field is shown for BP Tau (left hand panel) and V2129 Oph (right hand panel).

radii about the disc truncation radius calculated in §5.1. For V2129 Oph, where the disc truncation radius was calculated to be $2.8\,R_*$ (see Fig. 6), the accreting field is assumed to span the range of radii $\sim 2.4 - 3.2\,R_*$; for BP Tau, with a disc truncation radius of $\sim 4.8\,R_*$, accretion is assumed to occur from $\sim 4.4{-}5.2\,R_*$. In practise little difference is found in the structure of the accreting field when these values are varied. Figs. 7 and 8 also show the behaviour of a dipole magnetic field, tilted by 10°for comparison with the BP Tau data (whose dipole component is tilted by 10°relative to the stellar rotation axis), and by 30°for comparison with the V2129 Oph data.

Plots such as Figs. 7 and 8 allow a comparison of how the field complexity varies with height above the stellar surface. We note, however, that we do not account for how the structure of the magnetic field will evolve in time due to the interaction with the disc. However, this will be less of an issue if accretion proceeds from close to corotation, where the differential rotation of field line footpoints anchored in the disc and on the stellar surface is much less than if the disc is truncated well within corotation. As the strength of the dipole component decreases with height more slowly than the higher order field components, the behaviour of the field on the largest scales should be somewhat simpler than that of the surface field. This is the case for the magnetic field of V2129 Oph where the field behaves more like a dipole above $\sim 2.5R_*$ (see Fig. 7, right panel), after an initial fast drop within the strong complex field region close to the stellar surface. For BP Tau the field is generally more dipolar, even closer to the stellar surface (see Fig. 7, left panel), reflecting the much stronger dipole component of it's magnetic field, found to be 1.2 kG and containing about 50% of the magnetic energy (Donati et al. 2008a). For V2129 Oph if we assume that accretion occurs from around the disc truncation radius as calculated in the previous section, see Fig. 8, we find that the structure of the accreting field is much more complex than a simple dipole. Donati et al. (2007) found that the bulk of accretion in the visible hemisphere of V2129 Oph occured into a single magnetic spot at high latitude. Using the algorithm discussed in Gregory et al. (2007) and Jardine et al. (2008) we calculate that about 45% of the mass supplied by the disc would accrete into the high latitude northern hemisphere spot on V2129 Oph, with a similiar amount to an unseen southern hemisphere spot, and less than 10% to smaller equatorial spots. Thus, provided that the source surface is set to a large enough radius to allow the longest field lines to connect to the high latitude spot, the bulk of the accreting material accretes into the high latitude spots, even if the disc is truncated within the corotation radius.

6 CONCLUSIONS AND DISCUSSION

By extrapolating the fields of two T Tauri stars from observationally derived surface magnetograms we have compared the resulting magnetic field topologies with a simple dipole. We have found that although the surface magnetic fields of both stars are particularly complex, the larger scale field is simpler and more well ordered. This is consistent with previously published spectropolarimetric studies of accreting T Tauri stars, which suggested that bundles of accreting field lines connect to the stellar surface in single polarity regions, and were therefore likely well-ordered (e.g. Valenti & Johns-Krull 2004). The larger scale field of BP Tau in particular is closely matched to a dipole magnetic field, although V2129 Oph still shows departures from a dipole field even on the largest scales. However, for both stars, the footpoint separation at the stellar surface of the largest scale field lines is greater than for a purely dipolar magnetic field. In other words as the largest scale field lines arrive at the stellar surface, their structure is influenced by the much stronger field regions. The effect of this is that the largest scale field connects to the star at higher latitudes than would be expected when using a dipole magnetic field model. Thus by considering complex magnetic field topologies we find that the fractional open flux through the stellar surface is less than would be expected from dipole field models. The reduction in the fractional open flux is mainly attributable to the larger closed flux for the complex fields, which arises due to the numerous small magnetic loops close to the stellar surface. For both V2129 Oph and BP Tau there is less total open flux than for a dipole field, however, the difference is small enough (see Fig. 5) that there is unlikely to be any significant implications for the amount of angular momentum that can be carried away from such systems by a stellar wind (Matt & Pudritz 2005b, 2008a,b). However, more spectropolarimetric data for many different T Tauri stars will be required to confirm this.

If the extent of stellar magnetospheres are limited to well within corotation then accretion may proceed along the more complex regions of the stellar surface field. The result of this would be the formation of many low-latitude accretion hotspots (Gregory et al. 2005, 2006a). There is at least one star which shows evidence for such equatorial spots, GQ Lup (Broeg et al. 2007). However, for V2129 Oph and BP Tau the spectroscopic data of Donati et al. (2007, 2008a) clearly showed that the bulk of accreting material is carried into high latitude regions of the stellar surface. In order to explain such high latitude hotspots, Donati et al. (2007) and Jardine et al. (2008) demonstrated that for V2129 Oph the source surface must be set to at least $6.0\,R_*$, while for BP Tau the stellar magnetosphere must extend to at least $4\,R_*$ (Donati et al. 2008a). Selecting the location of the source surface sets the structure of the stellar magnetic field, although the inner disc may still be truncated closer to the stellar surface. Using the assumption that inner disc is located at the point where the torque due to viscous processes in the disc is comparable to the magnetic torque due to the stellar magnetosphere we estimated the disc truncation radius using the extrapolated fields. For BP Tau we found that the inner disc would be truncated close to the radius predicted for a dipole field, whereas for V2129 Oph, the inner disc is likely to be closer to the star. However, with large uncertainties in the assumed mass accretion rate (which influences the torque due to viscous processes in the disc), and with the static field structures considered here, such calculations are only of qualitative value. Further 3D MHD simulations, such as those already performed by, for example Long et al. (2008), are required in order to model how magnetic fields with an observed degree of complexity can disrupt and influence the structure of planet forming discs, and will represent a major future development in this field.

Although the radius of the source surface is essentially a free parameter of our model, the observed hotspot locations provide constraints. Once the source surface has been selected, however, this then also sets the structure of the X-ray emitting surface field, allowing predictions to be made regarding the stellar X-ray emission properties (Jardine et al. 2008). Such predictions will allow direct testing of our field extrapolation model with future independently obtained X-ray observations. A further test of the model will be the simulation of accretion related emission line profiles, and are currently being undertaken.

V2129 Oph, despite its young age, is massive enough to have developed a radiative core. In contrast to this BP Tau is likely to be completely convective. Although the field of BP Tau is more complex than a dipole, it is much simpler than that of V2129 Oph. The differences in the field structure of both stars likely reflect the different internal structure and the process by which their magnetic fields are generated and maintained. For stars with radiative cores the magnetic field is likely generated in the shear layer between the core and the outer convective envelope. In the absence of such a shear layer, it is difficult to explain how fully convective stars can generate and maintain large-scale almost axisymmetric kilo-Gauss fields, although recent theoretical models suggest that this is possible (Browning 2008). With only three magnetic surface maps available to date, V2129 Oph and two of BP Tau (Donati et al. 2007, 2008a), it is not possible to determine whether this is a general feature of all T Tauri stars, however it is similar to what it found for low mass main sequence stars (Donati et al. 2008b). More magnetic surface maps of T Tauri stars with varying stellar parameters are now required to test these ideas fully, and are an essential requirement to advance our understanding of stellar magnetism on the pre-main sequence.

ACKNOWLEDGEMENTS

The authors wish to thank the anonymous referee for comments which have helped to clarify a number of detailed points within this paper.

REFERENCES

Altschuler M. D., Newkirk G., 1969, SoPh, 9, 131

Azevedo R., Calvet N., Hartmann L., Folha D. F. M., Gameiro F., Muzerolle J., 2006, A&A, 456, 225

Beristain G., Edwards S., Kwan J., 2001, ApJ, 551, 1037

Bessolaz N., Zanni C., Ferreira J., Keppens R., Bouvier J., 2008, A&A, 478, 155

Bouvier J., 2007, in Bouvier J., Appenzeller I., eds, IAU Symposium Vol. 243 of IAU Symposium, The rotational evolution of young low mass stars. pp 231–240

Bouvier J., et al. 2007, A&A, 463, 1017

Broeg C., Schmidt T. O. B., Guenther E., Gaedke A., Bedalov A., Neuhäuser R., Walter F. M., 2007, A&A, 468, 1039

Browning M. K., 2008, ApJ, 676, 1262

Chuntonov G. A., Smirnov D. A., Lamzin S. A., 2007, Astronomy Letters, 33, 38

Clarke C. J., Armitage P. J., Smith K. W., Pringle J. E., 1995, MNRAS, 273, 639

Collier Cameron A., Campbell C. G., 1993, A&A, 274, 309

Donati J.-F., et al. 2007, MNRAS, 380, 1297

Donati J.-F., et al. 2008a, MNRAS, 386, 1234

Donati J.-F., et al. 2008b, MNRAS, submitted

Edwards S., Hartigan P., Ghandour L., Andrulis C., 1994, AJ, 108, 1056

Eisner J. A., Hillenbrand L. A., White R. J., Akeson R. L., Sargent A. I., 2005, ApJ, 623, 952

Favata F., Flaccomio E., Reale F., Micela G., Sciortino S., Shang H., Stassun K. G., Feigelson E. D., 2005, ApJS, 160, 469

Ferreira J., Dougados C., Cabrit S., 2006, A&A, 453, 785

Ferreira J., Pelletier G., Appl S., 2000, MNRAS, 312, 387

Flaccomio E., Micela G., Sciortino S., Feigelson E. D., Herbst W., Favata F., Harnden Jr. F. R., Vrtilek S. D., 2005, ApJS, 160, 450

Fleck R. C., 2008, Ap&SS, 313, 351

Getman K. V., Feigelson E. F., Broos P. S., Micela G., Garmire G. P., 2008a, ApJ, submitted

Getman K. V., Feigelson E. F., Micela G., Jardine M. M., Gregory S. G., Garmire G. P., 2008b, ApJ, submitted

Gregory S. G., Jardine M., Cameron A. C., Donati J.-F., 2006b, MNRAS, 373, 827

Gregory S. G., Jardine M., Collier Cameron A., Donati J.-F., 2005, in Favata F., et al. eds, Proceedings of the 13th Cambridge Workshop on Cool Stars, Stellar Systems and the Sun, held 5-9 July, 2004 in Hamburg, Germany. Edited by F. Favata et al. ESA SP-560, European Space Agency, 2005., p.191 Vol. 13, Accretion channeling in classical T Tauri stars. pp 191–+

Gregory S. G., Jardine M., Simpson I., Donati J.-F., 2006a, MNRAS, 371, 999

Gregory S. G., Wood K., Jardine M., 2007, MNRAS, 379, L35

Gullbring E., Hartmann L., Briceno C., Calvet N., 1998, ApJ, 492, 323

Hartmann L., Hewett R., Calvet N., 1994, ApJ, 426, 669

Hussain G. A. J., van Ballegooijen A. A., Jardine M., Collier Cameron A., 2002, ApJ, 575, 1078

Jardine M., Cameron A. C., Donati J.-F., Gregory S. G., Wood K., 2006, MNRAS, 367, 917

Jardine M. M., Gregory S. G., Donati J.-F., 2008, MNRAS, 386, 688

Johns-Krull C. M., 2007, ApJ, 664, 975

Johns-Krull C. M., Valenti J. A., Hatzes A. P., Kanaan A., 1999a, ApJL, 510, L41

Johns-Krull C. M., Valenti J. A., Koresko C., 1999b, ApJ, 516, 900

Königl A., 1991, ApJL, 370, L39

Küker M., Henning T., Rüdiger G., 2003, ApJ, 589, 397

Kurosawa R., Harries T. J., Symington N. H., 2006, MNRAS, 370, 580

Lin D. N. C., Bodenheimer P., Richardson D. C., 1996, Nature, 380, 606

Liu Y., Lin H., 2007, ApJ, submitted (astro-ph/0710.3223), 710

Long M., Romanova M. M., Lovelace R. V. E., 2005, ApJ, 634, 1214

Long M., Romanova M. M., Lovelace R. V. E., 2007, MNRAS, 374, 436

Long M., Romanova M. M., Lovelace R. V. E., 2008, MNRAS, 386, 1274

Mahdavi A., Kenyon S. J., 1998, ApJ, 497, 342

Matt S., Pudritz R. E., 2005a, MNRAS, 356, 167

Matt S., Pudritz R. E., 2005b, ApJL, 632, L135

Matt S., Pudritz R. E., 2008a, ApJ, 678, 1109

Matt S., Pudritz R. E., 2008b, ApJ, in press (astro-ph/0801.0440)

Mohanty S., Jayawardhana R., Basri G., 2005, ApJ, 626, 498

Muzerolle J., Calvet N., Hartmann L., 2001, ApJ, 550, 944

Najita J., Carr J. S., Mathieu R. D., 2003, ApJ, 589, 931

Riley P., Linker J. A., Mikić Z., Lionello R., Ledvina S. A., Luhmann J. G., 2006, ApJ, 653, 1510

Robitaille T. P., Whitney B. A., Indebetouw R., Wood K., 2007, ApJS, 169, 328

Romanova M. M., Lovelace R. V. E., 2006, ApJL, 645, L73

Romanova M. M., Ustyugova G. V., Koldoba A. V., Lovelace R. V. E., 2004, ApJ, 610, 920
Romanova M. M., Ustyugova G. V., Koldoba A. V., Wick J. V., Lovelace R. V. E., 2003, ApJ, 595, 1009
Shu F., Najita J., Ostriker E., Wilkin F., Ruden S., Lizano S., 1994, ApJ, 429, 781
Siess L., Dufour E., Forestini M., 2000, A&A, 358, 593
Simon M., Dutrey A., Guilloteau S., 2000, ApJ, 545, 1034
Symington N. H., Harries T. J., Kurosawa R., Naylor T., 2005, MNRAS, 358, 977
Terquem C., Papaloizou J. C. B., 2000, A&A, 360, 1031
Valenti J. A., Johns–Krull C. M., Hatzes A. P., 2003, in Brown A., Harper G. M., Ayres T. R., eds, The Future of Cool-Star Astrophysics: 12th Cambridge Workshop on Cool Stars, Stellar Systems, and the Sun (2001 July 30 - August 3), eds. A. Brown, G.M. Harper, and T.R. Ayres, (University of Colorado), 2003, p. 729-734. Vol. 12, Time Series Spectropolarimetry of T Tauri Stars. pp 729–734
Valenti J. A., Johns-Krull C. M., 2004, Ap&SS, 292, 619
van Ballegooijen A. A., Cartledge N. P., Priest E. R., 1998, ApJ, 501, 866
Wang Y.-M., 1996, ApJL, 465, L111+
Willis D. M., Young L. R., 1987, Geophysical Journal International, 89, 1011

This paper has been typeset from a TEX/ LATEX file prepared by the author.